

pubs.acs.org/Macromolecules Article

Modeling Phase Separation of Free-Radical Polymerizations in Crosslinked Networks

Adam L. Dobson, Sijia Huang, and Christopher N. Bowman*



Cite This: *Macromolecules* 2024, 57, 894–902



Read Online

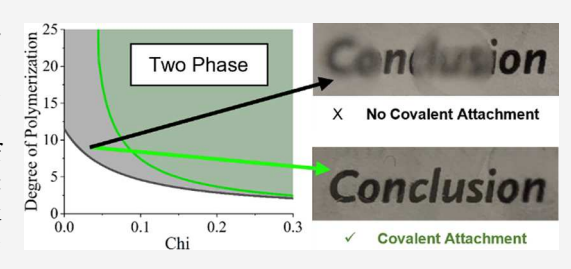
ACCESS I

III Metrics & More

Article Recommendations

Supporting Information

ABSTRACT: Herein, a thermodynamics model based on Flory—Rehner theory is used to predict conditions at which phase separation becomes thermodynamically favored in two-stage polymerization systems with wide utility in optical materials, membranes, and other porous materials. Methods for reduction of the Flory—Huggins interaction parameter and adjustment of component volume fractions are introduced to account for the covalent attachment of a growing polymer chain in the second phase to the network backbone formed in the first stage. The model predicts a delay in phase separation with an increase in covalent attachment, enabling larger Flory—



Huggins interaction parameters, larger degrees of polymerization, and larger monomer loadings to be used before phase separation becomes favorable as desired in various applications such as holography. The model is validated against coupled FTIR and UV—vis experiments and found to follow experimental phase diagram behavior with a slight underestimation of conversion at which phase separation begins to occur. The model provides a tool for monomer, network, and polymerization selection without the need for extensive trial-and-error experimentation.

■ INTRODUCTION

Two-stage polymerizations have found extensive use in the field of polymeric materials. In particular, two-stage polymerizations are common in lithography, shape memory and fixity, additive manufacturing, holography, and interpenetrating networks (IPNs). 1,2 For a two-stage polymerization, two orthogonal polymerization chemistries with orthogonal stimuli or disparate time scales are present together in a resin. A first stimulus is applied to react one set of monomers into a loosely crosslinked network, followed by the introduction of a second stimulus or longer time-scale reaction to create a subsequent, independent polymerization in the system. This process allows for a material to exhibit one set of properties early in its lifetime and a second set of properties for end-use at later times. This two-step polymerization scheme has been shown to be useful in improving initial handling characteristics, attaining greater final mechanical properties, and offering spatiotemporal control of optical, thermophysical, and viscoelastic properties.

One significant obstacle in two-stage polymerizations is polymerization-induced phase separation (PIPS), particularly during the second polymerization. As the second-stage polymerization occurs, enthalpic and entropic penalties to mixing are introduced, leading to a thermodynamic driving force for phase separation at some critical conversion for many of these systems. This behavior can create spatial variation in the composition of the final material. Although controlled PIPS is desirable, particularly for the fabrication of porous membranes, unanticipated inhomogeneities limit performance.^{3,4} For applications where increased mechanical properties are desired, spatial inhomogeneities create sites of different

mechanical properties where fracture propagation and premature failure occurs. For optical applications, inhomogeneities can form light-scattering loci and regions of mismatched refractive index, causing the onset of haze and limiting optical transmission.

A more recent approach to overcoming the obstacle of phase separation has been the inclusion of second-stage reactive moieties on the backbone of the first-stage network. In such a system, the initial resin contains monomers that participate solely in the first-stage polymerization, monomers that participate solely in the second-stage polymerization, and a third component that has functional groups to enable it to participate in both stages of polymerization. An example of this third component is hydroxyethyl acrylate, which contains an alcohol functional group capable of thermally stimulated addition reactions with the matrix and an acrylate group capable of photoinitiated free-radical polymerizations. The result of this system design after first-stage polymerization is a network with pendant reactive groups that participate in the second polymerization and allow for covalent attachment to the network backbone (Figure 1). This formulation decreases the enthalpic and entropic penalties associated with second-

Received: September 5, 2023 Revised: January 4, 2024 Accepted: January 9, 2024 Published: January 23, 2024





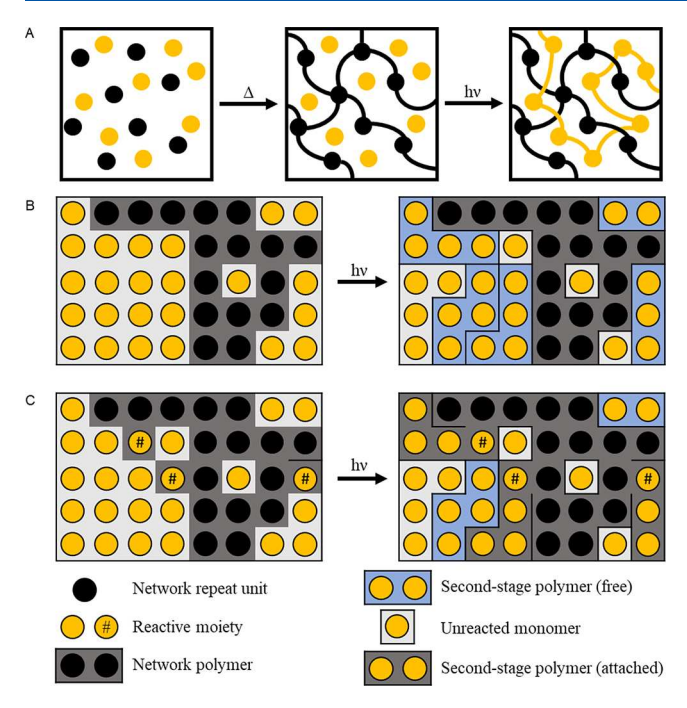


Figure 1. Schematic and lattice model for two-stage polymerization. (A) A monomer mixture is exposed to a stimulus (often thermal) to form a first-stage network. Upon exposure to a second stimulus (often light), a second polymerization occurs with the monomers that are unresponsive to the first stimulus. (B) Lattice representation of a traditional second-stage polymerization. Polymerization of monomer (light background) creates a large concentration of free polymer (blue background) in the system with respect to network concentration (dark background) and unreacted monomer. (C) With pendant reactive moieties on the network backbone (yellow circles with #), the concentration of free, unattached polymer is reduced, and the network becomes enthalpically more similar (more yellow units) to both free polymer and unreacted monomer.

stage polymerization and has been shown in holographic materials to dramatically reduce haze development. 5,6

An easily accessible, first-principles thermodynamic model to predict the onset of phase separation is a tool that would greatly enhance system design. The model must include configuration entropy of mixing, enthalpy of mixing, and entropy associated with the elasticity of the preformed network. Attempts to model phase separation phenomena during polymerization date back to the Flory-Rehner theory lattice model and Dušek. Dušek elucidated that diluent concentration and crosslinking density were vital factors in promoting phase separation in his systems.⁷ Boots et al. expanded Dušek's thermodynamic model to better include the effects of network elasticity in PIPS, in particular as applied to the formation of polymer-dispersed liquid crystals. This model simulated a single-stage polymerization where a mean-field approximation is used to distinguish between the fraction of reacted divinyl monomers that have formed an infinite network and the fraction that remain as free linear chains in the system. Later, Okay coupled thermodynamic equations based on the same Flory-Rehner model with reaction kinetics to determine gel point conversions that affect material properties and ultimately thermodynamic phase separation behavior. 9,10 Since then, a variety of models have been produced to simulate phase separation behavior, including density functional theorybased approaches and molecular dynamic simulations. 11-14

In this work, a first-principles model based on the works of Dušek and Boots is proposed. This model provides an intuitive understanding of the phase separation processes involved and is computationally simple. Although a thermal polymerization followed by photopolymerization is discussed and experimentally depicted here, the model readily applies to any combination of polymerizations where a polymer network is formed in the first stage and a free-radical, chain-growth mono(meth)acrylate polymerization is the second-stage polymerization. This model allows for the complex effects of covalent attachment of monomer and polymer to the backbone of the first-stage network, which has previously been ignored but has been shown to improve miscibility in two-stage polymerizations. The model provides tools for the rational design of a two-stage polymerization system that includes covalent attachment so as to promote or discourage phase separation at a desired conversion.

■ EXPERIMENTAL SECTION

Materials. Commercially available reagents were used without further purification. Reagent-grade triethylamine (TEA) was purchased from Fisher Scientific. Acryloyl chloride, dibutyl tin dilaurate (DBTDL), and 2-hydroxyethyl acrylate (HEA) were purchased from Sigma-Aldrich. Polycaprolactone-block-polytetrahydrofuran-blockpolycaprolactone (average Mn 2000) (Polyol 2000) was purchased from Sigma-Aldrich. 2,2-Dimethoxy-2-phenylacetophenone (DMPA) was purchased from TCI Chemicals. Desmodur N3900 triisocyanate (TriNCO) was donated by Covestro AG (formerly Bayer Material Science).

Sample Fabrication. Simulation predictions were compared to experimental phase separation behavior in a system applicable to holography (Figure 2). In this system, a mixture of dialcohol Polyol 2000, triisocyanate Desmodur N3900, 1-

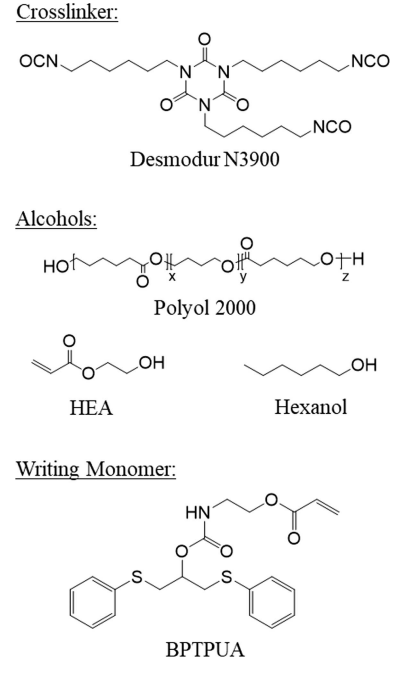


Figure 2. Monomers used for experimental validation. First-stage network is formed from crosslinker and alcohols. Inclusion of HEA enables covalent attachment during second-stage polymerization with BPTPUA.

hexanol, HEA, and second-stage writing monomer BPTPUA at 20, 30, or 40% loading was created with 1 wt % DMPA with respect to acrylate functional groups. Equimolar quantities of isocyanate functional groups and alcohol functional groups were used, and the ratio between monoalcohol (1-hexanol and HEA) and dialcohol (Polyol 2000) was kept consistent between groups to ensure similar crosslinking density of the first-stage network. The quantity of HEA was adjusted to create two groups for each monomer loading: one with $f_g = 0$ (no HEA) and one with $f_g = 0.10$. These mixtures were cast between glass slides at 250 μ m thickness, kept in the dark, and heated to 80 °C overnight to ensure complete first-stage polymerization, verified by the disappearance of an isocyanate peak in FTIR. No appreciable conversion of acrylate functional groups was noted during this process. Second-stage polymerization was conducted with 10 mW/cm² coherent LED light at 365 nm.

Experimental Setup. A dual UV-vis/FTIR setup was created using an optical bench. A light guide capable of transmitting broadband white light (400-800 nm) and UV light (365 nm LED) was positioned perpendicular to the sample to create a wide spot size, and light transmitted through the sample was captured by a UV-vis detector. At an angle to the sample was an FTIR light guide with a smaller diameter than the curing spot size, with its light captured by an FTIR detector. This enabled the calculation of acrylate conversion via the disappearance of its peak in the IR spectrum. A drop in white light transmission (taken at 575 nm, the peak in the broadband spectrum) was estimated to indicate the onset of phase separation in the sample. By coupling UV-vis transmission with FTIR, the critical conversion at which phase separation occurs (i.e., light transmission begins to drop) was experimentally determined.

MODEL DEVELOPMENT

A first-principles thermodynamic model for predicting phase separation in two-stage polymerizations was developed based on Flory–Rehner theory. In this system, a lattice model is assumed where phase separation occurs at compositions where the chemical potentials of the network-rich phase (gel phase, Phase I) are equal to the chemical potentials of the network-poor phase (sol phase, Phase II) for each component. According to Flory–Rehner theory, the Gibbs free energy of the system is described by the linear addition of all contributions to the Gibbs free energy. In the model proposed, the contributions to the total Gibbs free energy includes a Gibbs free energy of mixing $(\Delta G^{\rm mix})$, which consists of configurational entropy and enthalpy of mixing terms, and a Gibbs free energy associated with the elasticity of the prepolymerized network $(\Delta G^{\rm el})$:

$$\Delta G = \Delta G^{\text{mix}} + \Delta G^{\text{el}} \tag{1}$$

Both mixing and elastic contributions to the Gibbs free energy have been extensively studied and successfully used in predicting material behavior, most notably in hydrogel systems.

Chemical Potential due to Mixing. For a ternary system consisting of monomers that participate solely in the second-stage polymerization (subscript M), free polymer chains formed during the second-stage polymerization (subscript P), and crosslinked network formed during the first-stage polymerization with (in the case of covalent attachment) pendant second-stage polymer (subscript N), the Gibbs free energy of mixing has the following form:

$$\begin{split} \frac{\Delta G^{\text{mix}}}{Nk_{\text{B}}T} &= \frac{1}{r_{\text{M}}} \Phi_{\text{M}} \ln \Phi_{\text{M}} + \frac{1}{r_{\text{p}}} \Phi_{\text{p}} \ln \Phi_{\text{p}} + \frac{1}{r_{\text{N}}} \Phi_{\text{N}} \ln \Phi_{\text{N}} \\ &+ \chi_{\text{MP}} \Phi_{\text{M}} \Phi_{\text{P}} + \chi_{\text{MN}} \Phi_{\text{M}} \Phi_{\text{N}} + \chi_{\text{PN}} \Phi_{\text{P}} \Phi_{\text{N}} \end{split} \tag{2}$$

Here, $k_{\rm B}$ is Boltzmann's constant, T is temperature, r_i is the volume of component i measured in numbers of lattice sites, Φ_i is the volume fraction of component i, and χ_{ij} is the Flory–Huggins interaction parameter between component i and component j. N is the total volume of the phase (or, equivalently, the total number of lattice sites in the phase), and is given by the sum of the volumes of all components:

$$N = r_{\rm M}N_{\rm M} + r_{\rm P}N_{\rm P} + r_{\rm N}N_{\rm N} \tag{3}$$

where N_i is the total number of components i in the phase, such that r_iN_i is the volume of component i. The chemical potential in each phase for a given component is given by the partial derivative of the Gibbs free energy with respect to the number of that component (N_i) .

Taking the partial derivative of the Gibbs free energy with respect to $N_{M\nu}$ the chemical potential due to mixing for unreacted monomer can be obtained:

$$\frac{\Delta \mu_{\rm M}^{\rm mix}}{k_{\rm B}T} = \ln(\Phi_{\rm M}) + \left(1 - \frac{r_{\rm M}}{r_{\rm P}}\right) \Phi_{\rm P} + \left(1 - \frac{r_{\rm M}}{r_{\rm N}}\right) \Phi_{\rm N} + r_{\rm M} \chi_{\rm M} (1 - \Phi_{\rm M})^2 + r_{\rm M} \chi_{\rm P} \Phi_{\rm P}^2 + r_{\rm M} \chi_{\rm N} \Phi_{\rm N}^2 \tag{4}$$

The chemical potential for free growing polymer is obtained by exchanging indices M and P. Because $r_{\rm N}$ is the size of an infinite network, the term $\left(1-\frac{r_{\rm M}}{r_{\rm N}}\right)\Phi_{\rm N}$ reduces to $\Phi_{\rm N}$. An alternative form for the interaction parameters is used for ease of notation:

$$\chi_{\rm M} = \frac{1}{2} (\chi_{\rm MP} + \chi_{\rm MN}^{\rm eff} - \chi_{\rm PN}^{\rm eff}) \tag{5}$$

$$\chi_{\rm P} = \frac{1}{2} (\chi_{\rm MP} + \chi_{\rm PN}^{\rm eff} - \chi_{\rm MN}^{\rm eff}) \tag{6}$$

$$\chi_{\rm N} = \frac{1}{2} (\chi_{\rm MN}^{\rm eff} + \chi_{\rm PN}^{\rm eff} - \chi_{\rm MP}) \tag{7}$$

where $\chi^{\rm eff}$ is an effective interaction parameter with the network due to the enthalpic changes introduced by second-stage polymer covalent attachment to the first-stage network. For systems with no covalent attachment, $\chi^{\rm eff}_{ij}$ is χ_{ij} but in general changes with monomer loading and monomer conversion.

Chemical Potential due to Network Elasticity. The elastic contribution to the Gibbs free energy is provided by the following equation:

$$\frac{\Delta G^{\text{el}}}{Nk_{\text{B}}T} = \frac{\nu_{\text{e}}}{N} \left[\frac{3}{2} A \Phi_{\text{N}}^{2/3} \left(\left(\Phi_{\text{N}}^{\text{I}} \right)^{-2/3} - 1 \right) + B \ln \Phi_{\text{N}}^{\text{I}} \right]$$
(8)

Here, Φ_N is the volume fraction of the network during crosslink formation, related to monomer loading and solvent content; $\Phi_N^{\ \ I}$ is the volume fraction of the network in Phase I; A and B are constants pertaining to assumptions about the network and its connectivity; and ν_e is the number of elastically active chains in the network. For an ideal affine network made from step-growth polymerization of one diffunctional monomer species and one multifunctional monomer species, Flory

predicts that A=1 and B=2/f, where f is the functionality of the multifunctional monomer. This affine assumption is taken in this work to show qualitative trends in phase separation behavior. More complex elastic behavior is easily accommodated by simply replacing A and B with values more applicable to a particular system. For an ideal network where the total number of crosslinks remains unchanged, $v_{\rm e}=\frac{N^0\Phi_{\rm N}^{\alpha=0}}{m_{\rm e}}$, where $m_{\rm c}$ is the molecular weight (in lattice units) between crosslinks, N^0 is the system volume before swelling or deswelling, and $\phi_{\rm N}^{\alpha=0}$ is the volume fraction of the network before second-stage polymerization occurs. For a bulk system with negligible first-stage polymerization shrinkage, $\Phi_{\rm N}^{\alpha=0}=1-\Phi_{\rm M}^0$ for monomer loading volume fraction $\Phi_{\rm M}^0$. Taking the partial derivative with respect to number of monomer components provides the chemical potential change due to network elasticity for the monomer:

$$\frac{\Delta \mu_{\rm M}^{\rm el}}{k_{\rm B}T} = \left(\frac{\Phi_{\rm N}}{\Phi_{\rm N}^{\rm I}}\right)^{-1} (1 - \Phi_{\rm M}^{\rm 0}) \frac{r_{\rm m}}{m_{\rm c}} \left\{ A \left(\frac{\Phi_{\rm N}}{\Phi_{\rm N}^{\rm I}}\right)^{2/3} - B \right\} \tag{9}$$

An equivalent expression for free second-stage polymer formed is obtained by replacing $r_{\rm M}$ with $r_{\rm P}$.

Treatment of $\chi^{\text{eff.}}$ To use these expressions, an understanding of how network size grows and how χ changes with polymer addition to the network must be developed. To this end, three new parameters are defined. The first is f_g , the mole fraction of all reactive moieties that are present on the network. For a polymerization with one reactive moiety per monomer, f_g is defined as follows:

$$f_{\rm g} = \frac{N_{\rm moiety,N}}{N_{\rm moiety,N} + N_{\rm M}} \ll 1 \tag{10}$$

Assuming equal reactivity of the moieties on the network and the moieties present in monomer form, this fraction remains constant throughout the second-stage polymerization and represents a probability that a given reactive moiety will react with the network rather than a free monomer unit. From here, the probability (α_c) that a second-stage polymer consisting of r_P repeat units has attached to the network is determined from

$$\alpha_{\rm c} = 1 - (1 - f_{\rm g})^{r_{\rm p}} \tag{11}$$

This coupling variable represents the probability that at least one of the growing reactive units on the newly formed polymer has reacted with the network and has, therefore, covalently attached to it. Under the assumptions of equal reactivities of network and monomer moieties (f_g constant) and monodisperse polymer (r_p is constant), α_c is a constant.

The assumption of equal reactivities of moieties on the monomer and on the crosslinked network warrants further discussion. In general, the reactivities of free monomer double bonds and double bonds tethered to the crosslinked network need not be equal. This difference in reactivity arises from two sources. The first is inherent chemical differences in the reactive moieties themselves (e.g., a less reactive methacrylate moiety pendant from the network and a more reactive acrylate moiety in the free unreacted second-stage monomer). The second is differences in reactivity due to diffusion limitations. Because pendant moieties are tethered to a largely immobile network, their mobility is reduced compared to the free second-stage monomer. Therefore, when diffusion limitations

dominate reaction kinetics, moieties attached to the cross-linked network are expected to have lower reactivities than their free second-stage monomer counterparts. The effect is that, in general, parameters such as $f_{\rm g}$ and $r_{\rm P}$ are complex functions of time, conversion, local temperature, reaction kinetics, and second-stage monomer loading. To account for this variation in model parameters, a detailed understanding of kinetic coefficients, diffusion behaviors, free volume characteristics, and thermal properties for each component of the two-stage system under every examined photopolymerization condition may be leveraged to explicitly calculate model parameters at every point during photopolymerization.

In this work, the first-order approximation of constant f_{σ} is taken to introduce the mean-field thermodynamic model and demonstrate the model's utility for predicting phase separation in a wide variety of two-stage photopolymerizations, without the need for detailed kinetic knowledge of the system of interest. The assumption of constant f_g is valid when the reactivity of free second-stage monomers and the reactivity of pendant reactive moieties are approximately equal throughout the examined polymerization prior to phase separation. It is important to note that these reactivities need not be constant after phase separation and need only vary similarly during photopolymerization. Inherent chemical differences in reactivity are eliminated by use of identical reactive double bonds (e.g., acrylates) for both the moieties pendant from the network backbone and the moieties present in the free secondstage monomer. Differences in reactivity due to diffusion limitations are partially mitigated by focusing on systems that are reaction-limited (e.g., low crosslinking density, long network pendant moieties, high free volume) or propagationlimited (high crosslinking density, large second-stage monomer, low free volume) before phase separation. Although certain two-stage photopolymers may require a more nuanced treatment involving detailed and system-specific kinetics, the constant f_g assumption is reasonable for many applications, including most hydrogel, lithography, and holography systems.

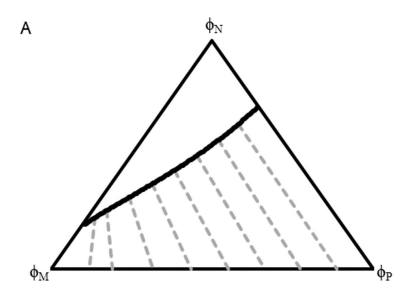
Assuming equal reactivities of moieties on the monomer and on the preformed network, the volume fractions of monomer, free second-stage polymer, and crosslinked network in the gel phase (Phase I) until the moment of phase separation are determined as functions of monomer loading, conversion, and $f_{\rm g}$:

$$\Phi_{\rm M}^{\rm I} = (1 - \alpha)\Phi_{\rm M}^0 \tag{12}$$

$$\Phi_{\rm p}^{\rm I} = \frac{1 - \alpha_{\rm c}}{1 - f_{\rm g}} \Phi_{\rm M}^0 \alpha \tag{13}$$

$$\Phi_{\rm N}^{\rm I} = 1 - \Phi_{\rm M}^0 + \frac{\alpha_{\rm c}}{1 - f_{\rm g}} \Phi_{\rm M}^0 \alpha - \frac{f_{\rm g}}{1 - f_{\rm g}} \Phi_{\rm M}^0 \alpha \tag{14}$$

A third parameter Φ_{PN} , the volume fraction of the network that contains incorporated second-stage polymer, is now determined:



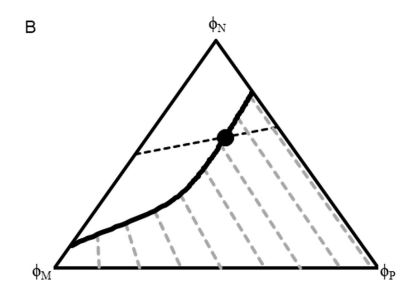


Figure 3. Phase diagrams of the three-component system. (A) Traditional ternary phase diagram. Solid black line indicates the phase separation boundary, with dotted gray lines tie lines. (B) Polymerization-phase diagram. Network properties change dynamically along a polymerization line (dotted black line) for a given monomer loading. The crossover (black dot) of a polymerization line with the phase separation boundary indicates the critical conversion at which phase separation becomes thermodynamically favored.

$$\begin{split} \Phi_{\text{PN}} &= \frac{\Phi_{\text{P}}^{\text{attached}}}{\Phi_{\text{N}}^{\text{I}}} \\ &= \frac{\frac{\alpha_{\text{c}}}{1 - \alpha_{\text{c}}} \Phi_{\text{P}}^{\text{I}}}{\Phi_{\text{N}}^{\text{I}}} \\ &= \frac{\alpha_{\text{c}} \Phi_{\text{M}}^{\text{0}} \alpha}{(1 - f_{\text{g}})(1 - \Phi_{\text{M}}^{\text{0}}) + (\alpha_{\text{c}} - f_{\text{g}}) \Phi_{\text{M}}^{\text{0}} \alpha} \end{split} \tag{15}$$

For the treatment of the interaction parameter evolution with polymer addition to the network, a method comparing Hildebrandt solubility parameters to χ is used. Given Hildebrandt solubility parameters, the interaction parameter between two components of a mixture is given by

$$\chi_{i,\text{solv}} = \frac{V_{\text{m,solvent}}}{RT} (\delta_i - \delta_{\text{solv}})^2 = \frac{r_{\text{solv}}}{k_B T} (\delta_i - \delta_{\text{solv}})^2$$
(16)

where $V_{\rm m,solv}$ is the molar volume over which relevant enthalpic interactions occur, traditionally taken to be the molar volume of the solvent; R is the universal gas constant; and δ_i is the Hildebrandt solubility parameter for component i. The righthand side of eq 16 is a conversion of units such that the terms match parameters in the model. The relevant molar volume for interaction $(r_{\rm solv})$ is taken to be the same for all species interactions, and the interaction parameters between all three species (free second-stage monomer M, free second-stage polymer P, and crosslinked network P0 are written as follows:

$$\chi_{\rm MN} = \frac{r_{\rm solv}}{k_{\rm B}T} (\delta_{\rm N} - \delta_{\rm M})^2 \tag{17}$$

$$\chi_{\rm MP} = \frac{r_{\rm solv}}{k_{\rm B}T} (\delta_{\rm P} - \delta_{\rm M})^2 \tag{18}$$

$$\chi_{\rm pN} = \frac{r_{\rm solv}}{k_{\rm B}T} (\delta_{\rm N} - \delta_{\rm p})^2 \tag{19}$$

From here, it is clear that the change in interaction parameter due to incorporation of second-stage linear polymer onto the network occurs because of a change in the network solubility parameter, $\delta_{\rm N}$. A group contribution method is used to determine the change in solubility parameter due to change in composition. If each lattice site is assumed to contribute equally to the solubility parameter, the resulting solubility parameter for the network is a volumetric average of the solubility parameters for the network initially and the solubility parameter of the added polymer:

$$\delta_{\rm N} = (1 - \Phi_{\rm PN})\delta_{\rm N}^{\,0} + \Phi_{\rm PN}\delta_{\rm P} \tag{20}$$

where $\delta_{\rm N}^0$ is the network solubility parameter before covalent attachment. Inserting this expression into the expressions for χ from Hildebrandt solubility parameters, the following relationships are obtained:

$$\chi_{\rm MP} = \chi_{\rm MN}^0 (1 - K)^2 \tag{21}$$

$$\chi_{\rm PN}^{\rm eff} = \chi_{\rm PN}^0 (1 - \Phi_{\rm PN})^2 \tag{22}$$

$$\chi_{\rm MN}^{\rm eff} = \chi_{\rm MN}^0 (1 - K\Phi_{\rm PN})^2 \tag{23}$$

$$K = \frac{\delta_{\rm N}^{0} - \delta_{\rm P}}{\delta_{\rm N}^{0} - \delta_{\rm M}} = \pm \sqrt{\frac{\chi_{\rm PN}^{0}}{\chi_{\rm MN}^{0}}}$$
(24)

The parameters χ^0 indicate interaction parameter values before any incorporation of a second-stage polymer. K is a constant relating the difference in solubility parameter of the initial crosslinked network and free second-stage polymer to the difference in solubility parameter of the initial crosslinked network and free second-stage monomer. If both polymer and monomer have solubility parameters larger or smaller than that of the network, this term is positive. Because the second-stage polymer is composed of monomer units, $\delta_{\rm M}$ and $\delta_{\rm P}$ are assumed to be similar in value, and so K is taken to be positive. It is worth noting that these equations have only two degrees of freedom. Therefore, once two interaction parameters are selected, the third is predetermined.

$$\Delta \mu_M^I = \Delta \mu_M^{II} \tag{25}$$

$$\Delta \mu_{P}^{I} = \Delta \mu_{P}^{II} \tag{26}$$

The final degree of freedom is taken as a free variable, used to determine phase separation characteristics at, for example, a specified monomer loading or conversion.

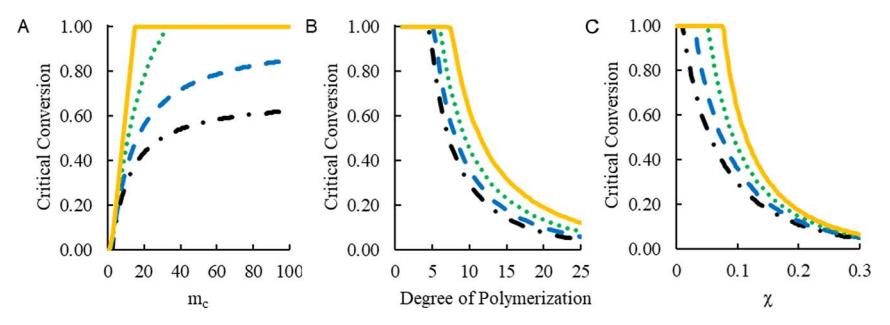


Figure 4. Predicted phase separation behavior as functions of key system parameters. Lines represent systems with no covalent attachment ($f_g = 0$, black dash-dot), $f_g = 0.01$ (blue dash), $f_g = 0.02$ (green dot), and $f_g = 0.03$ (yellow solid). Maximum conversion before phase separation is favored is depicted as a function of (A) molecular weight between crosslinks (m_c), (B) degree of polymerization (DP), and (C) Flory–Huggins interaction parameters (χ).

Ternary Phase Diagrams and Polymerization-Phase **Diagrams.** For a given system, ternary phase diagrams as well as conversions at which phase separation is thermodynamically favored are determined. A traditional ternary phase diagram for $\Phi_{\rm M}^{\ 0} = 0.5$ with covalent attachment ($f_{\rm g} = 0.03$) and monomer conversion of 0.53 is shown in Figure 3A. For a traditional ternary phase diagram, only the relative volume fractions of each component (monomer, free second-stage polymer, and crosslinked network) are considered. Each vertex indicates 100% of the labeled component, and the properties of each component are constant. The chemical potential contribution from elasticity takes the form of eq 9, where Φ_N is equal to Φ_N at the chosen monomer loading and conversion before swelling or deswelling occurs. For any system with $f_g > 0$, a degree of conversion from monomer to polymer must be first assumed to establish the properties of the network. Because network properties are assumed to be constant in traditional ternary phase diagrams, these diagrams cannot account for changes in phase behavior that arise as a result of evolving network features during cure.

Of particular interest is the determination of monomer loading and corresponding achievable monomer conversions during polymerization that are achieved before the onset of phase separation is favored. A traditional ternary phase diagram cannot show this behavior because the monomer conversion and monomer loading must be selected prior to diagram creation. To overcome this obstacle, a polymerization-phase diagram is proposed here (Figure 3B), with analogous diagrams present elsewhere in literature for similar systems. 8,15,16 In a polymerization-phase diagram, a series of monomer loadings is selected, and the points of phase separation along the corresponding polymerization lines are calculated. It is worth noting that in a system without covalent attachment, the polymerization line is a horizontal line across the diagram. For systems with $f_{\rm g}$ > 0, however, the polymerization line has a positive slope due to the increase in network volume as monomer conversion increases and a portion of the newly formed polymer becomes attached to the initial polymer network. As the degree of conversion from a selected monomer loading increases, network properties are allowed to change, and phase separation behavior is determined. The point where the polymerization line for a specified monomer loading and the phase separation boundary meet is the critical conversion. This critical conversion indicates the point at which phase separation is thermodynamically favorable.

Effect of Crosslinking Density, Degree of Polymerization, and Flory-Huggins Interaction Parameter on Phase Separation. From here, the effect of any relevant system property on critical conversion is calculated. In the plots that follow (Figures 3 and 4), all the model parameters used are $\varphi_{\rm M}^0 = 0.5$, $m_{\rm c} = 10$, $r_{\rm P} = 10$, $\chi_{\rm MP} = 0$, $\chi_{\rm MN}^0 = \chi_{\rm PN}^0 = 0.1$, and α_{crit} = 0.99, unless otherwise stated. Three system parameters are found to have a profound effect on the onset of phase separation. The first of these is crosslinking density, which is related to m_c and the elastic contribution to free energy (Figure 3A). In a traditional system without covalent attachment ($f_g = 0$, black lines in Figure 3), crosslinking density has a dramatic effect on achievable conversion before phase separation, with only very loosely crosslinked (high m_c) systems enabling high conversion of a single-phase system. The reason is that network elasticity introduces a free energy penalty for the existence of a single-phase system. With the inclusion of covalent attachment $(f_g > 0)$, the penalty from elastic energy is mitigated such that, for the system with $f_{\rm g}$ = 3% of reactive moieties on the network backbone, no phase separation is predicted when m_c is greater than approximately 10 monomer units. Despite no direct reduction in the elastic contribution, covalent attachment lowers the unfavorable free energy contributions from enthalpic interaction and configurational entropy significantly enough to partially offset the elastic

The next system parameter of interest is degree of polymerization (DP) of the second-stage polymer. In this model, the DP is equivalent to $\frac{r_p}{r_M}$, which reduces to r_p when r_M is assumed to be one lattice site. As DP increases, critical conversion expectedly decreases. For the traditional system with no covalent attachment, phase separation begins near DP = 4.5, whereas this is brought to the slightly higher value of DP = 7 for the system with f_g = 0.03. For a system with f_g > 0, a larger DP enables a greater extent of covalent attachment. The result is a system that has more favorable enthalpic interactions (χ reduction) and more favorable configurational entropy ($\varphi_{\rm P}^{\rm I}$ reduction) compared to its $f_g = 0$ counterpart. While increasing the critical DP from 4.5 to 7 may seem minimal, there are two important factors to consider. The first is that if moderate conversions (~20-30%) are permissible, the difference between systems with and without covalent attachment is greater. The second consideration is that the DP of free polymer chains is likely to be lower in systems that allow for covalent attachment than that for systems without covalent attachment. Mathematically, this is seen in the expression for $\alpha_{\rm c}$. Polymer chains with a lower $r_{\rm p}$ have a higher probability of

remaining free of the network compared to polymer chains with a higher r_p . The result is a skewing of the size of free polymer chains to lower values of DP when covalent attachment is possible.

The final parameter investigated that greatly influences phase separation is the Flory-Huggins interaction parameter. Because the second-stage polymer repeating units consist entirely of monomer, the enthalpic interaction between monomer and polymer is taken to be minimal, or $\chi_{\rm MP} \sim 0$, as a first approximation. For the model, this means that $\chi_{\rm MN}$ = χ_{PN} . Figure 3C shows the effect of χ_{MN} on critical conversion. In a traditional system, phase separation begins for $\chi \sim 0.01$, whereas phase separation only occurs in the f_g = 0.03 system for χ > 0.07, due to the combined effect of $\chi_{\rm MN}$ and $\chi_{\rm PN}$ reduction from covalent attachment and effective removal of free polymer from Phase I. The strength of this effect for systems with covalent attachment decreases as χ increases to large values. The reason for this behavior is that at high values of χ , phase separation occurs at conversions low enough that relatively few polymer chains attach to the network before phase separation (Figure S2.2). The result is that the effective χ values for interacting with the network do not change appreciably before phase separation is induced.

From here, a systematic guide for the selection of secondstage monomer and monomer loadings is developed. By selecting a desired monomer loading, desired monomer conversion, and molecular weight between crosslinks predetermined by first-stage polymerization chemistries, allowable degrees of polymerization and interaction parameters for the monomer are predicted.

Figure 4A shows a plot of DP and χ at the moment phase separation becomes thermodynamically favored for $f_g = 0$, $m_c =$ 10, $\alpha = 0.99$, and $\Phi_{\rm M}^{0} = 0.3$. Parameter space below the curve represents conditions that will not induce phase separation, while the parameter space above the curve shows conditions for which two phases are favorable. Figure 5B shows these same conditions but allowing for covalent attachment. As f_{σ} increases, a larger portion of the χ -DP parameter space is available before phase separation. This approach allows for a wider variety of monomer species and polymerization properties to be available, granting greater freedom in monomer selection for the two-stage polymerization. For example, for a chain-growth polymerization that achieves a DP of 11, the system without covalent attachment requires monomer-network and polymer-network enthalpic interactions to be negligible ($\chi = 0$), while a system with $f_g = 0.03$ enables monomer and network selection for χ values up to approximately 0.075.

Once a monomer and network are chosen, the maximum allowable monomer loading is predictable. Figure 4C shows these results for a monomer system with $r_{\rm P}=10$ and $\chi=0.1$, and a preformed network of $m_{\rm c}=10$. Under these conditions, a traditional network with no covalent attachment accommodates a volume fraction of 0.165 monomer loading before phase separation is favored during second-stage polymerization. With only 3 mol % of reactive moieties present on the network backbone ($f_{\rm g}=0.03$), phase separation is predicted never to become favorable until monomer loadings greater than 30% are used. Thus, a user has two new tools for two-stage polymerization design. The first is that, given a desired monomer loading, the available interaction (χ) and polymerization properties (DP) of a monomer to be selected are predetermined. The second is that, given a desired monomer

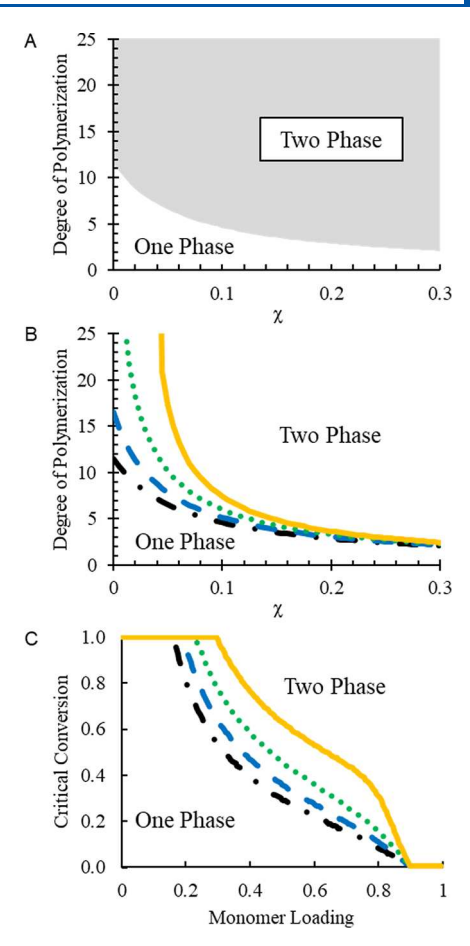


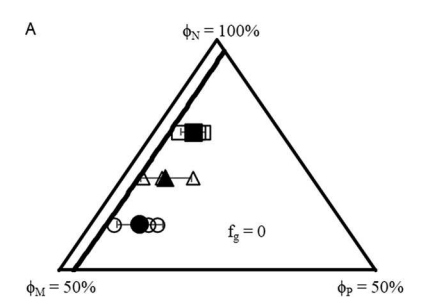
Figure 5. Allowable parameter space based on design specifications. Lines represent systems with no covalent attachment ($f_{\rm g}=0$, black dash-dot), $f_{\rm g}=0.01$ (blue dash), $f_{\rm g}=0.02$ (green dot), and $f_{\rm g}=0.03$ (yellow solid). For a given system with a desired conversion, combinations of degree of polymerization (DP) and Flory—Huggins interaction parameters (χ) uniquely define one-phase and two-phase regimes for (A) $f_{\rm g}=0$, and (B) various $f_{\rm g}$ values. (C) For a given system chemistry, desired conversion and maximum monomer loading uniquely define one-phase and two-phase regimes.

and polymerization system, the maximum allowable monomer loading is predetermined.

EXPERIMENTAL RESULTS FOR MODEL VALIDATION

Experimental measurements and model predictions for the onset of phase separation are seen in the polymerization-phase diagrams in Figure 6. These diagrams are truncated such that the bottom vertices indicate 50% of their corresponding components to focus the plots on the region of the diagram where experimental data was taken. The solid black line indicates model predictions for when phase separation is thermodynamically favored; the solid shapes indicate mean values; open shapes are individual data points, with different shapes indicating different monomer loadings. All model predictions are plotted with $m_c = 5$, $r_p = 9$, $\chi_{\rm MP} = 0$, $\chi_{\rm MN} = \chi_{\rm PN} = 0.21$, with only the value of $f_{\rm g}$ changing between the plots.

Model predictions for maximum conversion before the onset of phase separation are near but generally lower than the points where phase separation is observed to occur experimentally. This is an expected result, as the model predicts only when phase separation is thermodynamically favored, as it is not able



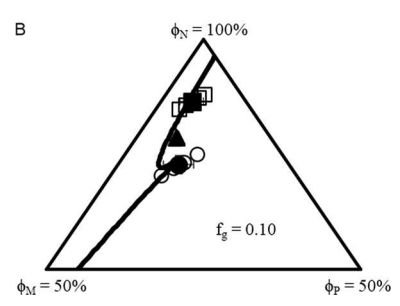


Figure 6. Truncated polymerization-phase diagrams for experimental validation. Individual data points (open shapes) and means (filled shapes) for 20% (square), 30% (triangle), and 40% (circle) monomer loadings are plotted with model predictions (black line) with (A) no covalent attachment and (B) covalent attachment allowed ($f_g = 0.10$).

to consider the kinetics and time scales necessary for phase separation to occur and form domains of size scales that scatter light. Specifically, for phase separation to occur, diffusive processes must subsequently occur to organize species into different domains. Because the process of domain formation, even when it is thermodynamically favorable is ultimately kinetically controlled, the thermodynamic model is unable to describe the size scales or time scales for achieving heterogeneities in the system. The result is that the model predicts when phase separation becomes thermodynamically favored but not the time at which light-scattering domains are large enough and concentrated enough to be detectable by UV-vis. Although the two-stage system selected was one experimentally observed to readily and rapidly form haze after phase separation, an inherent delay in experimental turbidity is inevitable compared to model predictions.

Still, the model accurately predicts a variety of aspects of the phase diagram. First, the model correctly identifies that phase separation occurs at lower conversions for a system without covalent attachment. Furthermore, the model predicts an unusual curvature in the phase diagram that is backed experimentally (Figure 6B). The reason for this curvature is that the addition of monomer into the system has competing effects. On one hand, greater monomer loading introduces a larger penalty for a single-phase system in terms of configurational entropy. At the same time, however, greater monomer loading enables larger extents of covalent attachment and, therefore, larger decreases in χ_{MN} and χ_{PN} as conversion increases. A balance between these competing thermodynamic forces is reached at some optimal monomer loading, which the model predicts.

CONCLUSIONS

A first-principles thermodynamic model based on Flory-Rehner theory is developed that predicts phase separation in two-stage polymerizations. Although lattice-model strategies have been used for similar purposes in the past, this model is the first one able to accommodate the covalent attachment of growing second-stage polymers onto a first-stage network. The model predicts that primary network crosslinking density (inverse of m_c), Flory-Huggins interaction parameters (χ), and DP strongly impact the tendency of a two-stage system to thermodynamically prefer phase separation. When covalent attachment of a growing second-stage polymer onto the firststage network is enabled via reactive moieties on the network backbone, the model predicts a larger parameter space available for network, monomer, and polymerization properties before phase separation is predicted to be thermodynamically preferred. Comparison of predicted polymerization-phase diagrams to diagrams constructed via haze detection validates the utility of the model in predicting the earliest possible onset of phase separation in these systems. This model enables users to know a priori if a selected two-stage polymerization system is likely to phase separate due to thermodynamic driving forces.

ASSOCIATED CONTENT

Supporting Information

The Supporting Information is available free of charge at https://pubs.acs.org/doi/10.1021/acs.macromol.3c01803.

Detailed model derivations and additional model results (PDF)

AUTHOR INFORMATION

Corresponding Author

Christopher N. Bowman — Department of Chemical and Biological Engineering, University of Colorado Boulder, Boulder, Colorado 80309, United States; orcid.org/0000-0001-8458-7723; Email: christopher.bowman@colorado.edu

Authors

Adam L. Dobson – Department of Chemical and Biological Engineering, University of Colorado Boulder, Boulder, Colorado 80309, United States

Sijia Huang – Department of Chemical and Biological Engineering, University of Colorado Boulder, Boulder, Colorado 80309, United States

Complete contact information is available at: https://pubs.acs.org/10.1021/acs.macromol.3c01803

Author Contributions

The manuscript was written through contributions of all authors. All authors have given approval to the final version of the manuscript.

Funding

Funding for this project was provided by NSF grant CHE 1808484.

Notes

The authors declare no competing financial interest.

REFERENCES

(1) Kuang, X.; Zhao, Z.; Chen, K.; Fang, D.; Kang, G.; Qi, H. J. High-Speed 3D Printing of High-Performance Thermosetting Polymers via Two-Stage Curing. *Macromol. Rapid Commun.* **2018**, 39 (7), No. 1700809.

- (2) Li, X.; Gai, Y.; Sun, M.; Li, Y.; Xu, S. Drum Tower-Inspired Kirigami Structures for Rapid Fabrication of Multifunctional Shape-Memory Smart Devices with Complex and Rigid 3D Geometry in a Two-Stage Photopolymer. *Adv. Funct. Mater.* **2022**, 32 (40), No. 2205842.
- (3) Tsai, J. T. Retainment of Pore Connectivity in Membranes Prepared with Vapor-Induced Phase Separation. *J. Membr. Sci.* **2010**, 362, 360–373.
- (4) Benmouna, F.; Maschke, U.; Coqueret, X.; Benmouna, M. Equilibrium phase behavior of polymer and liquid crystal blends. *Macromol. Theory Simul.* **2000**, *9* (5), 215–229.
- (5) Hu, Y.; Kowalski, B. A.; Mavila, S.; Podgórski, M.; Sinha, J.; Sullivan, A. C.; McLeod, R. R.; Bowman, C. N. Holographic Photopolymer Material with High Dynamic Range (Δn) via Thiol—Ene Click Chemistry. *ACS Appl. Mater. Interfaces* **2020**, *12* (39), 44103–44109.
- (6) Song, J.-S.; Tronc, F.; Winnik, M. A. Two-Stage Dispersion Polymerization toward Monodisperse, Controlled Micrometer-Sized Copolymer Particles. J. Am. Chem. Soc. 2004, 126 (21), 6562–6563.
- (7) Dušek, K. Phase Separation during the Formation of Three-Dimensional Polymers. J. Polym. Sci. Part C Polym. Symp. 1967, 16 (3), 1289–1299.
- (8) Boots, H. M. J.; Kloosterboer, J. G.; Serbutoviez, C.; Touwslager, F. J. Polymerization-Induced Phase Separation. 1. Conversion—Phase Diagrams. *Macromolecules* 1996, 29 (24), 7683—7689.
- (9) Okay, O. Phase Separation in Free-Radical Crosslinking Copolymerization: Formation of Heterogeneous Polymer Networks. *Polymer* **1999**, *40* (14), 4117–4129.
- (10) Okay, O. Macroporous Copolymer Networks. *Prog. Polym. Sci.* **2000**, 25 (6), 711–779.
- (11) Lee, J. C. Polymerization-Induced Phase Separation. *Phys. Rev.* E **1999**, *60* (2), 1930–1935.
- (12) Aguiar, L. G. A Cross-Linking Copolymerization Mathematical Model Including Phase Separation and Cyclization Kinetics. *Macromol. Theory Simul.* **2015**, 24 (3), 176–180.
- (13) Yandek, G. R.; Kyu, T. Theoretical Modeling of the Phase Separation Dynamics in Blends of Reactive Monomers. *Macromol. Theory Simul.* **2005**, 14 (5), 312–324.
- (14) Oya, Y.; Kikugawa, G.; Okabe, T.; Kawakatsu, T. Density Functional Theory for Polymer Phase Separations Induced by Coupling of Chemical Reaction and Elastic Stress. *Adv. Theory Simul.* **2022**, *5* (1), No. 2100385.
- (15) Chan, P. K.; Rey, A. D. Polymerization-Induced Phase Separation. 1. Droplet Size Selection Mechanism. *Macromolecules* **1996**, 29 (27), 8934–8941.
- (16) Kwok, A. Y.; Prime, E. L.; Qiao, G. G.; Solomon, D. H. Synthetic Hydrogels 2. Polymerization Induced Phase Separation in Acrylamide Systems. *Polymer* **2003**, *44* (24), 7335–7344.